


Network Pharmacology and Experimental Validation to Explore That Celastrol Targeting PTEN is the Potential Mechanism of *Tripterygium wilfordii* (Lév.) Hutch Against IgA Nephropathy

Juanyong Zhao , Haiyang Liu, Ming Xia, Qian Chen, Lili Wan, Bin Leng, Chengyuan Tang, Guochun Chen, Yu Liu, Lei Zhang, Hong Liu

Hunan Key Laboratory of Kidney Disease and Blood Purification, Department of Nephrology, The Second Xiangya Hospital, Central South University, Changsha, People's Republic of China

Correspondence: Hong Liu; Lei Zhang, Hunan Key Laboratory of Kidney Disease and Blood Purification, Department of Nephrology, The Second Xiangya Hospital, Central South University, Changsha, People's Republic of China, Tel +86-13973116951; +86-18673174522, Email liuhong618@csu.edu.cn; zhanglei_xp@163.com

Purpose: Accumulating clinical evidence showed that *Tripterygium hypoglaucum* (Lév.) Hutch (THH) is effective against IgA nephropathy (IgAN), but the mechanism is still unclear. This study is to evaluate the renal protective effect and molecular mechanism of THH against IgAN via network pharmacology, molecular docking strategy and experimental validation.

Methods: Several databases were used for obtaining the active ingredients of THH, the corresponding targets, as well as the IgAN-related genes. The critical active ingredients, functional pathways, and potential for the combination of the hub genes and their corresponding active components were determined through bioinformatics analysis and molecular docking. The IgAN mouse model was treated with celastrol (1 mg/kg/d) for 21 days, and the aggregated IgA1-induced human mesangial cell (HMC) was treated with various concentrations of celastrol (25, 50 or 75 nM) for 48 h. The immunohistochemistry and Western blot techniques were applied to evaluate the protein expression of the predicted target. The cell counting kit 8 (CCK8) was used to detect HMC proliferation.

Results: A total of 17 active ingredients from THH were screened, covering 165 IgAN-related targets. The PPI network identified ten hub targets, including PTEN. The binding affinity between the celastrol and PTEN was the highest (−8.69 kJ/mol). The immunohistochemistry showed that celastrol promoted the expression of PTEN in the glomerulus of IgAN mice. Furthermore, the Western blot techniques showed that celastrol significantly elevated the expression of PTEN and inhibited PCNA and Cyclin D1 in vitro and in vivo. The CCK8 assay determined that celastrol decreased HMC proliferation in a concentration-dependent manner.

Conclusion: This study suggests that activating PTEN by celastrol may play a pivotal role in THH alleviating IgAN renal injury.

Keywords: IgA nephropathy, *Tripterygium hypoglaucum* (Lév.) Hutch, network pharmacology, molecular docking, celastrol, PTEN

Introduction

IgA nephropathy (IgAN) is the most prevalent primary glomerular disease. The detection rate of renal biopsy in China is as high as 28.1%, which accounts for 40% of primary glomerular diseases in Asia.^{1,2} The characteristic of IgAN is IgA deposition in the glomerular mesangial area, proliferation of the mesangial cell, and expansion of the matrix. There is persistent hematuria with or without proteinuria, hypertension, and edema in the clinical manifestations of IgAN. Moreover, 30–40% of IgAN patients will have impaired renal function.³ However, there is a lack of targeted treatment for primary IgAN. The therapeutic schedule recommended in the KDIGO 2021 guidelines is focused on conventional therapy, including the application of angiotensin receptor blocker (ARB) or angiotensin-converting enzyme inhibitor (ACEI), appropriate control of blood pressure, a limited salt diet and proper aerobic exercise.⁴ The utilization of corticosteroids and other immunosuppressive therapies is partly limited in the treatment of IgAN. Therefore, advancing

more effective and secure medicines to treat IgAN is very imperative. Many IgAN patients turn to traditional Chinese medicine and achieved good curative effects.⁵

Tripterygium hypoglaucum (Levl.) Hutch (THH) is a plant of the genus *Tripterygium* belonging to the Euonymus family, with a similar pharmacological action as *Tripterygium wilfordii* Hook F (TwHF). Some researchers consider that TwHF and THH are the same species based on DNA sequencing technology.^{6,7} However, their composition and toxicity are slightly different, some scholars believe that the toxicity and side effects of THH are less than TwHF.^{8,9} Due to its striking immunosuppressive and resist-inflammatory effects, THH is applied extensively in many kinds of immune system diseases such as rheumatoid arthritis, psoriasis, and diabetic kidney disease, which can exert its pharmacological effects through multiple targets and multiple pathways.^{10–12} As preparations of dried root extract of THH, Colquhounia Root Tablet and Kunxian Capsule have been used for treating kinds of kidney disease in China for over 30 years because of their favorable clinical effects and medicinal value.¹³ However, the pharmacological mechanisms of THH in IgAN have not been fully understood yet.

Different from one-to-one drug and drug target reaction research, network pharmacology provides a more complex prospect of pharmacological action based on public databases with available pharmacological data, protein–protein interaction data, and genetic–disease associations.¹⁴ Molecular docking is a medicinal screening and designing method. It could calculate the affinity and simulate the interaction between the drug molecules and the receptor macromolecules based on computer simulation technology.¹⁵ In this study, the targets of the major bioactive ingredients of THH and the susceptibility targets of IgAN were collected using the network pharmacology method. The biological enrichment analyses of overlapping targets were utilized to find out the potential molecular mechanism of THH against IgAN. The “Herb–Ingredient–Target” network and protein–protein interaction (PPI) network were conducted. The molecular docking technology was applied for verifying the binding potential of the top ten hub targets and their corresponding active components. Finally, the mouse and cell models of IgAN were established and treated with celastrol. The expression of the major predicted protein was further validated via immunohistochemistry and Western blot techniques. The cell counting kit 8 (CCK8) was used to detect HMC proliferation. A flowchart of this study is shown in Figure 1.

Materials and Methods

Network Pharmacology Research

Collection of Main Active Components of *Tripterygium hypoglaucum* (Lév.) Hutch and Correlated Targets

The components of THH were collected via the Traditional Chinese Medicine Systems Pharmacology Database (TCMSP, <http://tcmsp.com/tcmssp.php>) which has collected more than 500 kinds of herbs and 1000 kinds of chemical compositions registered in Chinese Pharmacopoeia (2015 edition). Moreover, the components were supplemented by literature searching.¹⁰ Based on ADME (absorption, distribution, metabolism and excretion) screening method, oral bioavailability (OB) $\geq 30\%$ and drug-likeness (DL) ≥ 0.18 were used as the filtering criteria for effective active ingredients.¹⁶ Simultaneously, the potential targets associated with active ingredients of THH were screened with the TCMSP, supplemented by Swiss Target Prediction platform (<http://www.swisstargetprediction.ch/>), and PubChem database (<https://pubchem.ncbi.nlm.nih.gov/>).

Screening of the Targets Related to IgAN

The IgAN target genes were identified by retrieving public databases including Online Mendelian Inheritance in Man (OMIM, <https://omim.org/>) and GeneCards (<https://www.genecards.org>). Both databases are authoritative research resources on human genes, phenotypes and diseases.^{17,18} All research involving human data, including publicly available data from databases, were approved by the Ethics Committee of the Second Xiangya Hospital of Central South University (Approval No. 2021SNK1123000).

Construction and Analysis of the “Herb–Ingredient–Target” Network

The common targets of IgAN and the effective active ingredients were identified with Venn diagrams and visualized by bioinformatics (<http://www.bioinformatics.com.cn>), an online platform for data analysis and visualization. And the “Herb–Ingredient–Target” network was established through Cytoscape software (Version 3.8.2, <https://www.cytoscape.org/>).

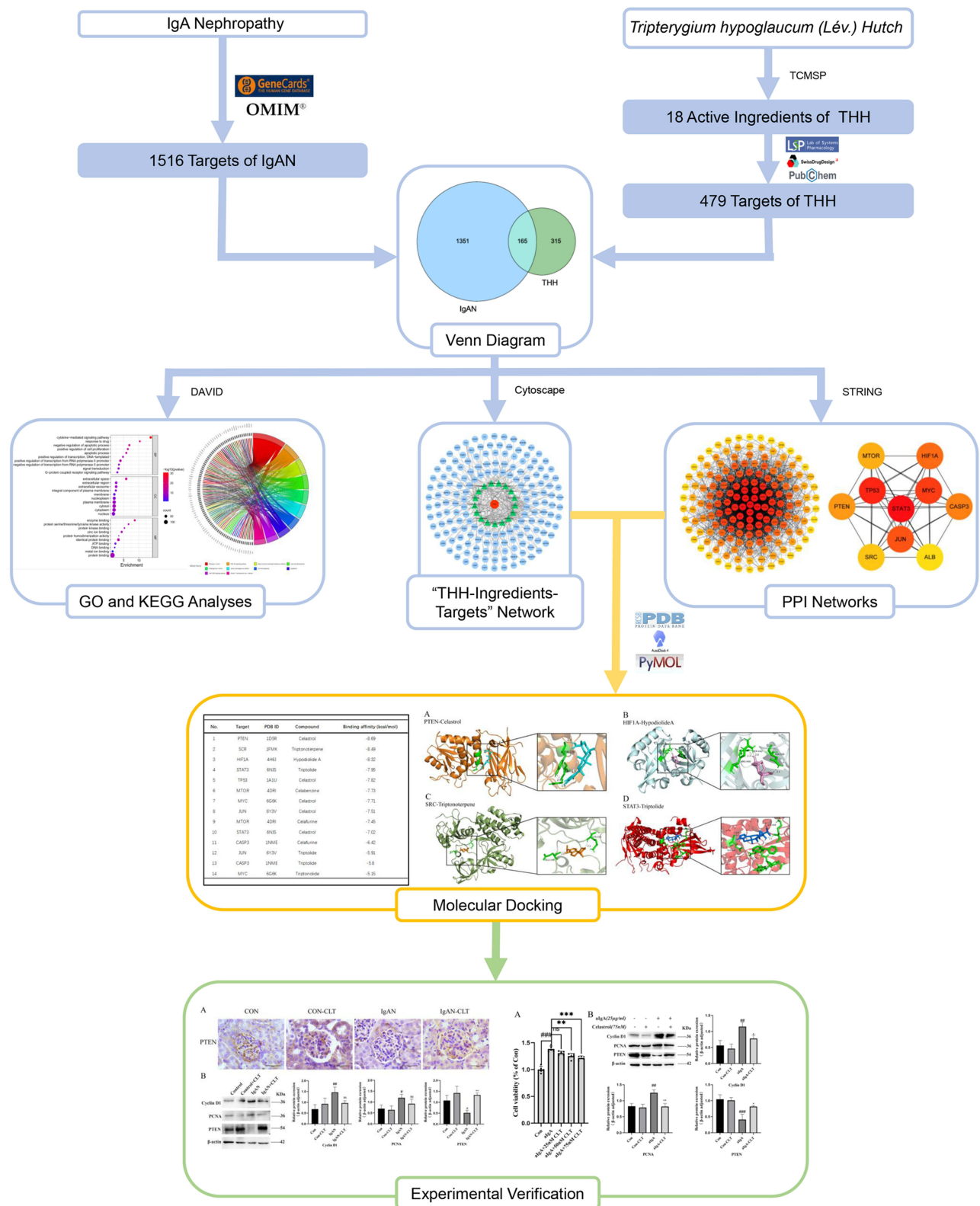


Figure 1 Network pharmacology, molecular docking, and experimental verification workflow for identifying *Tripterygium hypoglaucum* (Lév.) Hutch targets the treatment of IgA Nephropathy. *p < 0.05 vs control group, **p < 0.01 vs control group, ***p < 0.001 vs control group, #p < 0.05 vs IgAN OR IgA group, ##p < 0.01 vs IgAN group, ns: p > 0.05 vs Control OR IgAN OR IgA group.

GO and KEGG Pathway Enrichment Analyses

To identify the underlying mechanisms of the common targets of THH and IgAN, the GO enrichment and KEGG signaling pathway analysis were analyzed using Database for Annotation, Visualization, and Integrated Discovery (DAVID, <https://david.ncifcrf.gov>) website. The p -value < 0.05 was defined as the critical value of significant enrichment.

Construction and Analysis of Protein–Protein Interaction Network

A Protein–Protein Interaction (PPI) network map was constructed for understanding the co-expression, function, interaction, and dynamical aspects of potential targets.¹⁹ The overlapping targets of THH and IgAN were imported into the STRING database (<https://string-db.org/>).²⁰ Unconnected single proteins were removed. The PPI diagram of these targets was imported into Cytoscape 3.8.2 for visual analysis. The CytoHubba plug-in unit was used to screen the core targets in the PPI network, and the high-accuracy Maximal Clique Centrality (MCC) method was selected to score the core degrees.

Molecular Docking Analysis

The top ten core targets in the PPI network and associating ingredients were selected for molecular docking. The 3D structures of candidate active compounds were downloaded from the PubChem (<https://pubchem.ncbi.nlm.nih.gov/>), and the OpenBabel software was used for converting them to the PDB format. The crystal structure of hub protein was obtained in the Protein Data Bank (PDB, <https://www.rcsb.org/>). The AutoDock Tools 1.5.6 software was used to remove water molecules, add hydrogenate and save recipients and ligands in the PDBQT format. Finally, the Autodock Vina 1.1.2 was used for performing molecular docking and calculating the binding affinity. Each docking calculation produced 10 structures, and the molecular docking output was prioritized according to the frequency of possible ligand-binding sites and free energy score. The docking results of core proteins and related active components were visualized by PyMOL 2.2.0 software.

Experimental Verification

Experimental Animals and Drug Treatments

Twenty male C57BL/6J mice (weighing 22 ± 2 g and about 6–8 weeks old) were purchased from Cyagen Biosciences Inc (China, License number: SCXK-(Su)2018–0003) and were raised in a specific pathogen-free condition with the appropriate temperature, humidity and a 12 h light/dark cycle. Animals were given free access to water and a standard laboratory diet. All animal experiment protocols followed the national guidelines of laboratory animal welfare, reviewed and approved by the Institutional Animal Care and Use Committee at the Second Xiangya Hospital, Central South University (Approval No. 2021509).

After adaptive feeding for one week, the mice were randomly divided into four groups, including the control group (Control), the IgAN group (IgAN), the control group treated with celastrol (Control-CLT), and the IgAN group treated with celastrol (IgAN-CLT). The mouse model of IgAN was induced as previously described.²¹ In brief, BSA (Sigma) dissolved in 0.16% hydrochloric acid solution (800 mg/kg) was administered by gavage once every other day, and CCl₄ dissolved in castor oil (1:5) was injected subcutaneously weekly (0.08 mL) and intraperitoneal biweekly (0.1 mL). At weeks 6 and 8, LPS (Sigma) (50 μ g) was injected through the tail vein. One mouse in each group was executed early, and IgA deposition in the glomeruli was visualized through direct immunofluorescence to examine whether the model was established successfully. The establishment of the IgAN model was finished at the end of the 10th week. From the 7th week, mice received celastrol (Selleck, NSC70931, Shanghai, China, 1 mg/kg/d, dissolved in 0.01% dimethyl sulfoxide) intraperitoneal injection or saline for 21 days.²² After the intervention ended, all mice were anesthetized with pentobarbital and euthanasia by cervical dislocation. The renal tissue of mice was collected for subsequent experiments.

Immunohistochemical Staining

Formaldehyde-fixed and paraffin-embedded mice renal tissues were sliced into 4 μ m sections. After deparaffinized and rehydration, slides in heated citrate buffer were subjected to antigen retrieval. Then, the slides were exposed to primary

antibody (PTEN 1:200, Proteintech, 22034-1-AP) at 4°C overnight. Then, the tissues were incubated with HRP-linked secondary antibody and stained with DAB kit (Vector Laboratories). The slides were visualized under light microscopy (Nikon Tokyo, Japan). All the analyses were repeated more than three times. The representative images are displayed.

Cell Culture and Treatment

The Human Glomerular Mesangial Cell (HMC CBR130735), purchased in CellBiolabs, were cultured in (DMEM)/F-12 medium (Gibco) supplemented with 10% fetal bovine serum (FBS, Gibco, USA), 100 µg/mL streptomycin and 100 U/mL penicillin (Thermo Fisher) at 37°C and 5% CO₂. aIgA1 was obtained by aggregating Monomeric human IgA1 (Abcam, USA) at 65°C for 150 min on a plate heater, as previously described.²³ The celastrol (Selleck) was dissolved in dimethyl sulfoxide (DMSO) to prepare a stock solution. Cells were incubated with aIgA1 alone or with a combination of celastrol (0–75 nM) concentrations for 48 h.

CCK-8 Assay

Cell proliferation was detected by Cell Counting Kit-8 (CCK8) assay (Dojindo) following the recommended procedure of the manufacturer. In brief, cells were seen in a 96-well culture plate at a density of 5000 cells per well. After cells were incubated at 37°C for 24 hours, aIgA1 alone or in combination with celastrol (0, 25, 50, and 75 nM) was added to treat cells for 48 hours. And then 10 µL of CCK8 was added per well. The absorbance was detected at 450 nm using a Microplate Reader (Molecular Devices, Biorad).

Western Blot Analysis

The cells and renal tissues were lysed in RIPA Lysis buffer (Beyotime Biotechnology, China) supplemented with PMSF. Then, the lysate was disintegrated three times by ultrasound and centrifuged at 1200 g for 10 min at 4°C to obtain the supernatants. The protein levels were measured using the BCA protein assay kit (Thermo Fisher). The samples were electrophoresed by SDS-PAGE and transferred to PVDF membranes. After blocking with 5% BSA at room temperature for 1 h, the membranes were incubated overnight at 4°C with the primary antibodies: PTEN (1:10000, Abcam, ab267787), Cyclin D1 (1:10000, Abcam, ab134175), PCNA (1:20000, Proteintech, 10205-2-AP). After incubation with horseradish peroxidase (HRP)-conjugated secondary antibodies (goat anti-rabbit IgG H&L and goat anti-mouse IgG H&L, Proteintech, SA00001-2, SA00001-1) at room temperature for 1 hour, the blots of protein were visualized with an enhanced chemiluminescence kit (Millipore).

Statistical Analysis

Data are presented as the mean ± SD. The Kruskal–Wallis test and Dunn’s pairwise comparison test were used to analyze the differences between multiple groups. All experiments were independently repeated at least three times, and statistical significance was set at $p < 0.05$. All statistical analyses were performed using GraphPad Prism 8.0 software.

Results

Active Components and Related Targets of THH

The main ingredients of THH were screened from the TCMSP databases and previous literature. There were 149 ingredients identified from THH ([Table S1](#)). Based on criteria with OB ≥ 30% and DL ≥ 0.18, [Table 1](#) lists 18 vital active components including triptolide, celastrol, triptonoditerpenic acid and others. As shown in [Table S2](#), the results of retrieval from TCMSP, PubChem, and Swiss Target Prediction suggested that a total of 479 targets were linked to the 18 active compounds of THH.

Acquisition of IgAN Disease Targets

To identify the viral genes involved in the IgAN glomerular injury, IgAN-related targets were collected from OMIM and Gene Card databases. Using “IGA Nephropathy OR Glomerulonephritis, IGA OR Berger’s Disease” as the keywords, 1516 IgAN-related genes were obtained ([Table S3](#)).

Table 1 The 18 Vital Active Components of *Tripterygium hypoglaucum* (Lév.) Hutch and Their ADME (Absorption, Distribution, Metabolism, and Excretion) Characteristics

Mol ID	Molecule Name	OB (%)	DL	Molecular Formula
MOL000492	(+)-catechin	54.83	0.24	C ₁₅ H ₁₄ O ₆
MOL003225	Hypodiolide A	76.13	0.49	C ₂₀ H ₃₀ O ₃
MOL003224	Triptidolnide	56.4	0.67	C ₂₀ H ₂₄ O ₆
MOL003187	Triptolide	51.29	0.68	C ₂₀ H ₂₄ O ₆
MOL003192	Triptonide	67.66	0.7	C ₂₀ H ₂₂ O ₆
MOL003245	Triptonoditerpenic acid	42.56	0.39	C ₂₁ H ₂₈ O ₄
MOL003280	Triptonolide	49.51	0.49	C ₂₀ H ₂₂ O ₄
MOL005314	Celabenzine	101.88	0.49	C ₂₃ H ₂₉ N ₃ O ₂
MOL003208	Celafurine	72.94	0.44	C ₂₁ H ₂₇ N ₃ O ₃
MOL003229	Triptinin B	34.73	0.32	C ₂₀ H ₂₆ O ₃
MOL003231	Triptoditerpenic acid B	40.02	0.36	C ₂₁ H ₂₈ O ₃
MOL003248	Triptonoterpene	48.57	0.28	C ₂₀ H ₂₈ O ₂
MOL000073	(+)-Epicatechin	48.96	0.24	C ₁₅ H ₁₄ O ₆
MOL003196	Triptophenolide	48.5	0.44	C ₂₀ H ₂₄ O ₃
MOL003186	Celastrol	17.84	0.78	C ₂₉ H ₃₈ O ₄
MOL006791	Epigallocatechin	24.18	0.27	C ₁₅ H ₁₄ O ₇
MOL000263	Oleanolic acid	29.02	0.76	C ₃₀ H ₄₈ O ₃
MOL003278	Salaspermic acid	32.19	0.63	C ₃₀ H ₄₈ O ₄

“THH-Ingredient-Target” Network Construction

The Venn diagrams showed overlapping targets related to both THH and IgAN (Figure 2A), and the 165 common targets were obtained for subsequent analysis. The network of interactions between 165 overlapping genes and 17 compounds was constructed by Cytoscape 3.8.2 software and consisted of 183 nodes and 312 edges (Table S4, Figure 2B). In this network, the red polygon represented the THH, the green triangles represented the active components, and the blue circles represented the targets. The lines stood for interactions between the targets and the chemical component.

Functional Enrichment Analysis

To reveal the potential mechanism underlying the therapeutic effect of THH in IgAN, GO and KEGG pathway analyses of the 165 common targets were performed via DAVID functional annotation tools. By GO enrichment analysis, 774 GO items were significantly enriched ($p < 0.05$), including 589 biological process (BP), 63 cellular component (CC) and 122 molecular function (MF) terms. GO functional enrichment bubble diagram (Figure 3A) shows the top 10 enriched BPs, CCs and MFs. The bubble size indicated the number of enriched targets in the relevant pathways. And color represented $-\log_{10}(p\text{-value})$. The bigger the bubble, the more targets were enriched. And bigger $-\log_{10}(p\text{-value})$ was represented by a redder color. The BPs enriched mainly in the Positive regulation of transcription from RNA polymerase II promoter pathway, Cytokine-mediated signaling pathway, Signal transduction, Negative regulation of apoptotic process, and so on. The CCs were mainly related to the Cytosol, Cytoplasm, Nucleus, and Postsynaptic membrane. The MFs were mostly related to Protein binding, Identical protein binding and Zinc ion binding. Detailed information on the GO analysis

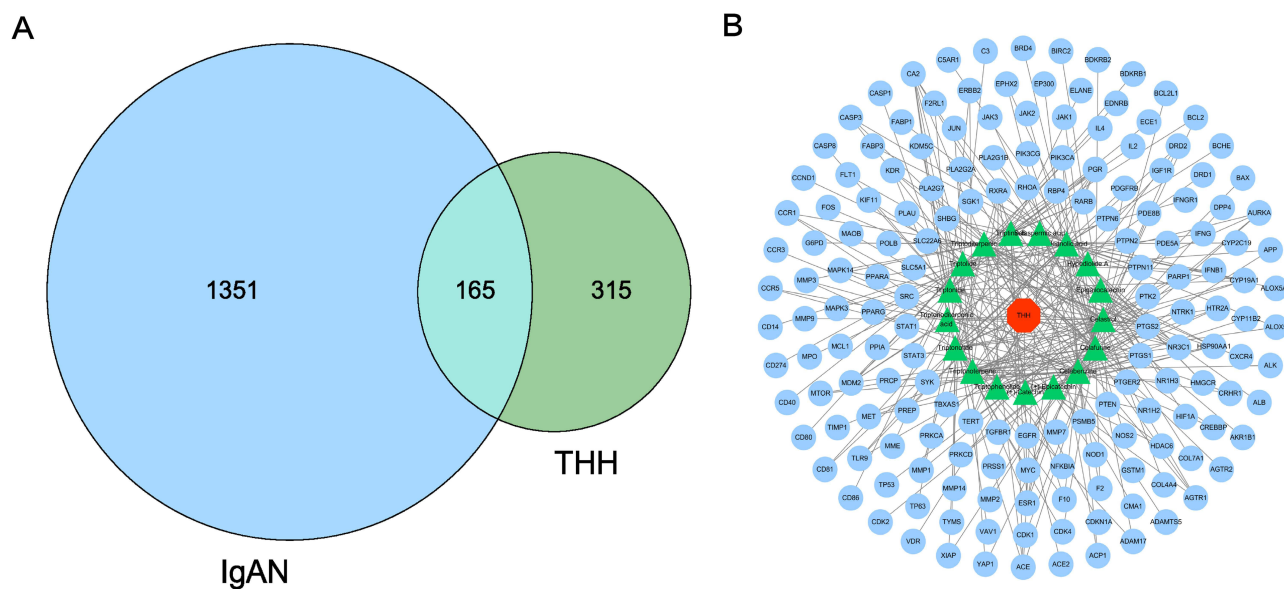


Figure 2 The network model of *Tripterygium hypoglaucomum* (Lév.) Hutch in the treatment of IgA Nephropathy. **(A)** There are 165 common potential targets related to THH and IgAN. **(B)** The network model of vital active components and targets. The red polygons represent the THH, the green triangles represent the active components, the blue circles represent the targets, and the lines represent the interaction relationships.

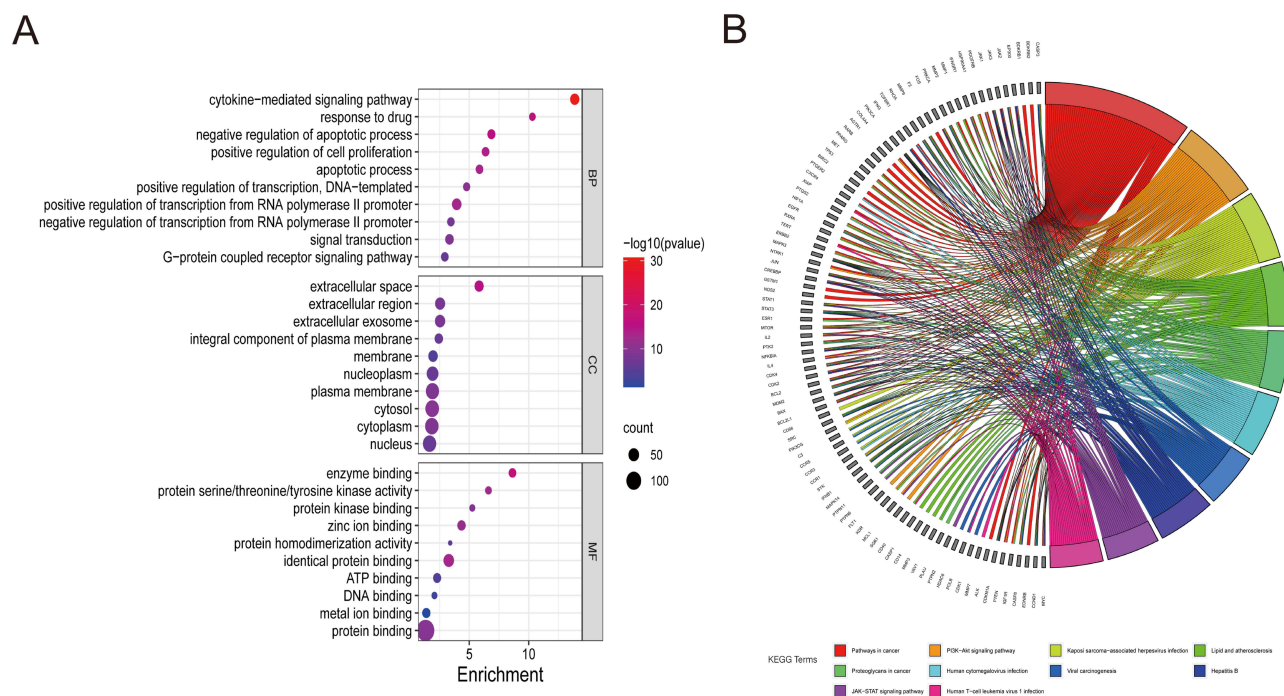


Figure 3 GO and KEGG functional pathway enrichment analyses. **(A)** Top 10 GO analyses of the biological process (BP), cellular component (CC), and molecular function (MF). The color scale of the bubble chart indicates the p-value, and the dot size means the gene count in each term. **(B)** Top 10 results of KEGG pathway enrichment analyses and the related genes.

results was provided in [Table S5](#). A total of 154 KEGG pathways were significantly enriched ($p < 0.05$). [Figure 3B](#) shows the top 10 biological pathways including the Pathways in cancer, PI3K-Akt signaling pathway, Kaposi sarcoma-associated herpesvirus infection pathway, Lipid and atherosclerosis pathway, Proteoglycans in cancer pathway and other signaling pathways. Other related pathways are listed in [Table S6](#).

PPI Network Construction and Hub Targets Recognition

The 165 IgAN-THH common targets were analyzed using a PPI network constructed by the STRING database. The PPI network included 163 nodes and 2656 edges, in which each node represented a protein, and each edge represented a functional association between potential targets. Two nodes (SLC22A6 and PDE8B) were removed since they were not attached to other nodes in the network. The PPI network was imported into Cytoscape 3.8.2 for further analysis. The core targets were screened with the CytoHubba plugin. The redder the color of representative nodes, the more important the position of proteins in the network (Figure 4A). As shown in Figure 4B, 10 hub targets were recognized, including STAT3, TP53, MYC, JUN, HIF1A, CASP3, PTEN, MTOR, SRC, and ALB.

Prediction of Hub Target–Compound Interaction by Molecular Docking

Based on the PPI network and “Herb-ingredient-target” network, the top 10 targets and their corresponding active components were selected for molecular docking using Autodock. The lower the binding energy, indicating the greater the binding affinity between the target and ligand, and the more stable the binding. The binding energy is lower than -5 kJ/mol indicating good interaction.²⁴ Fourteen pairs of target components can be well binding. The results of binding affinity are shown in Table 2. Using PyMOL, the three-dimensional view of the top 4 docking mode with the highest binding energy are displayed in Figure 5.

Interestingly, the binding affinity of celastrol and PTEN is the highest (-8.69 kJ/mol). In addition, celastrol is the active ingredient of THH that matches the greatest number of targets in the core PPI network (Table S4). Therefore, experiments were conducted to verify whether celastrol affects the PTEN-related signaling pathway.

Celastrol Promoted the Expression of PTEN and Inhibited the Expression of PCNA and Cyclin D1 in IgAN Mice

To verify the expression of PTEN in the glomerulus of mice, immunohistochemical analyses were conducted in renal tissue samples from the mice in the control group, IgAN group, control group treated with celastrol, and IgAN group treated with celastrol. As shown in the immunohistochemical results, compared with Control, PTEN was remarkably decreased in the renal glomerular of IgAN mice, while treated with celastrol recovered PTEN expression (Figure 6A).

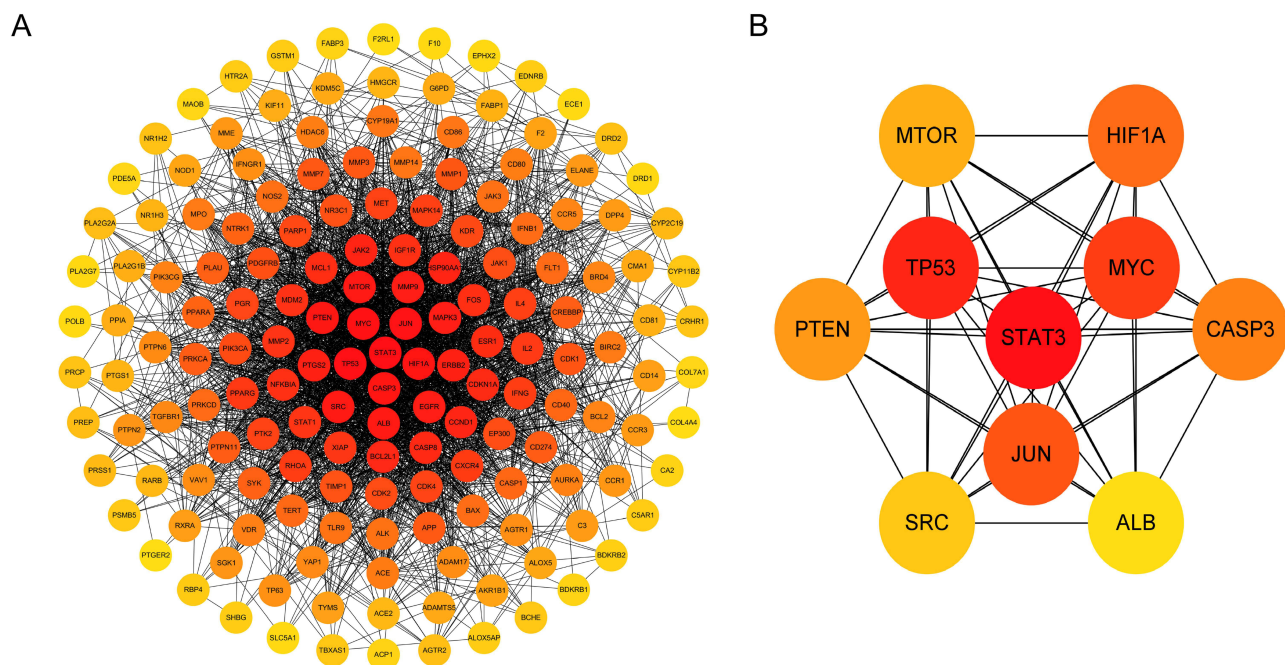


Figure 4 The PPI network and the key genes of the IgAN-THH common targets. **(A)** PPI network of candidate targets of THH against IgAN. The redder the node, the more important the targets in the network. **(B)** The map of the central top 10 targets network.

Table 2 Molecular Docking Results of Top 10 Targets and Corresponding Active Components. The Binding Affinity Arrayed from High to Low

No.	Target	PDB ID	Compound	Binding Affinity (kcal/mol)
1	PTEN	1D5R	Celastrol	-8.69
2	SRC	1FMK	Triptonoterpene	-8.49
3	HIF1A	4H6J	Hypodiolide A	-8.32
4	STAT3	6NJS	Triptolide	-7.95
5	TP53	1A1U	Celastrol	-7.82
6	MTOR	4DRI	Celabenzine	-7.73
7	MYC	6G6K	Celastrol	-7.71
8	JUN	6Y3V	Celastrol	-7.51
9	MTOR	4DRI	Celafurine	-7.45
10	STAT3	6NJS	Celastrol	-7.02
11	CASP3	1NME	Celafurine	-6.42
12	JUN	6Y3V	Triptolide	-5.91
13	CASP3	1NME	Triptolide	-5.8
14	MYC	6G6K	Triptonolide	-5.15

The Western blot detection of renal cortex tissue proteins also confirmed that celastrol elevated PTEN. The expression of Cyclin D1, a member of the cyclin family that participated in regulating the progress of the cell cycle, and PCNA, another marker of cell proliferation, was also measured. Both declined following celastrol treatment (Figure 6B).

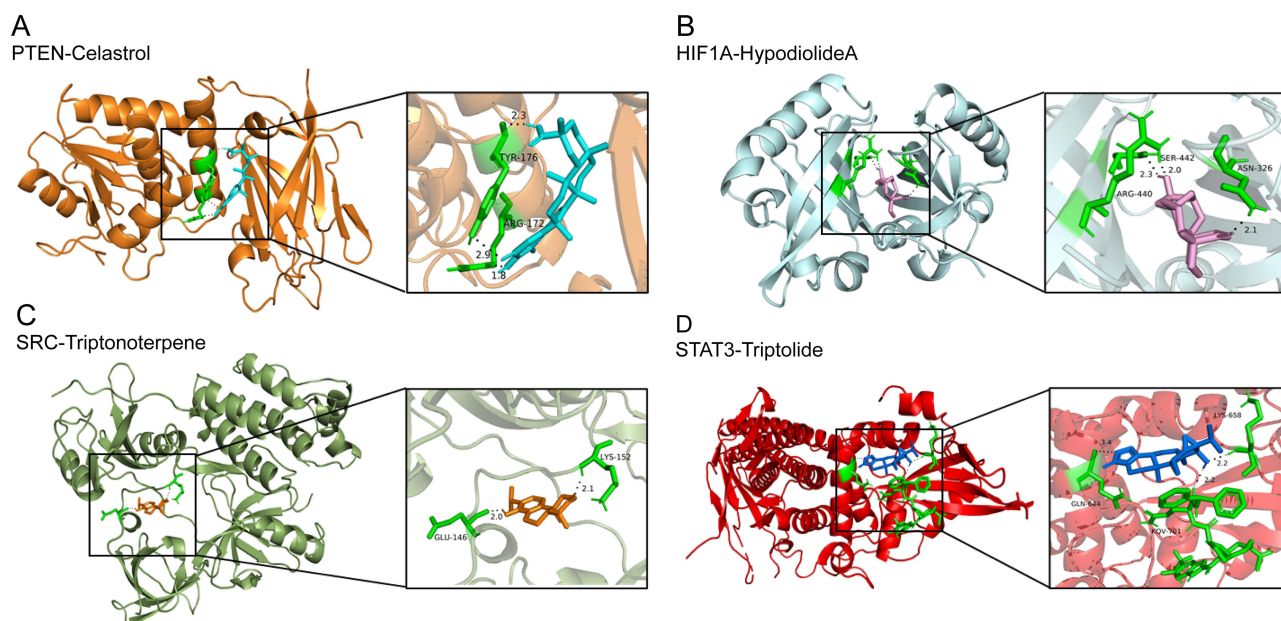


Figure 5 3D Docking conformations of the targets and the THH components with top 4 binding energy. (A) Celastrol and PTEN, (B) Hypodiolide A and HIF1A, (C) Triptonoterpene and SRC, (D) Triptolide and STAT3.

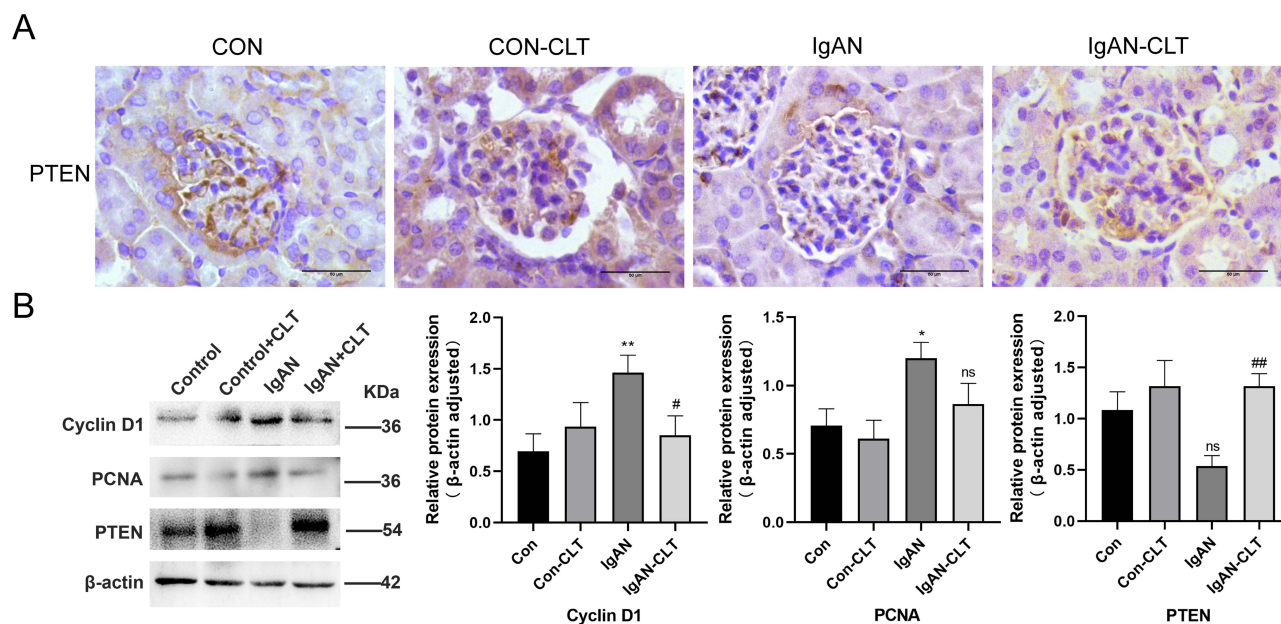


Figure 6 Celastrol upregulated PTEN signaling in the kidney of IgAN mice. **(A)** Representative images of glomerular immunohistochemical staining with PTEN in Celastrol treated mice or control mice. Bars=50μm. Images were captured at ×400 magnification. **(B)** Western blot and gray value statistics of PTEN, Cyclin D1 and, PCNA in renal cortex tissue samples. All data presented as mean ± SD, n=6. *p < 0.05 vs control group, **p < 0.01 vs control group, #p < 0.05 vs IgAN group, ##p < 0.01 vs IgAN group, ns: p > 0.05 vs Control OR IgAN group.

Celastrol Prevented alGA-Induced HMC Proliferation and Regulated the Expression of PTEN, PCNA and Cyclin D1

The HMC was stimulated with 25 μg/mL aIgA1 to construct the IgAN vitro model, as previously reported.²³ We investigated whether celastrol prevented alGA-induced HMC proliferation effectively. The CCK8 analysis showed that celastrol attenuated cell proliferation in a concentration-dependent manner after 48 hours of intervention (Figure 7A). The alGA1 induced a decrease in the protein level of PTEN and increase the expression of Cyclin D1 and PNCA protein; while treated with celastrol, the change was reversed (Figure 7B). These results suggest that celastrol is a potent cell proliferation inhibitor in alGA1-stimulated HMC.

Discussion

IgAN is a leading cause of ESRD in adults. Without effective intervention, it will cause irreversible renal dysfunction and a high dialysis rate,²⁵ resulting in loss of labor force and a serious social burden.²⁶ Exploring the mechanism of therapy and prevention of IgAN has become growingly essential. Glomerular inflammation and immune disorder of IgAN have been indicated to contribute to cellular proliferation, glomerulosclerosis and tubulointerstitial fibrosis, leading to disease progression and loss of renal function.²⁷ This means that medicine with anti-inflammatory and immunomodulatory effects may be a promising candidate for the treatment of IgAN.

In the research of treatment of kidney disease, *Tripterygium* relates drugs have been proven to be effective in reducing proteinuria, improving renal function, and lowering the recurrence rate, in the meanwhile, the incidence of adverse reactions.^{13,28,29} In the study of mechanism, the pharmacological effect of *Tripterygium* component is mainly reflected in anti-inflammatory and immune regulation, including regulating MAPK³⁰ and TLR4/NF-κB³¹ classic inflammation signal pathway, declining the NLRP3 inflammasome,³² and improving the Oxidative Stress.³³ MAPK/ERK pathway has been proved to play a significant role in the injury of IgAN mesangial cells.³⁴ Recently, we found that Triptolide, a monomer component in *Tripterygium*, is an autophagy promoter to inhibit mesangial cell proliferation in IgAN via the CARD9/p38 MAPK pathway.²¹ In the current study, we performed using network pharmacology and molecular docking technology to describe a comprehensive and integrated prospect of the mechanisms of *Tripterygium*-based traditional Chinese medicine

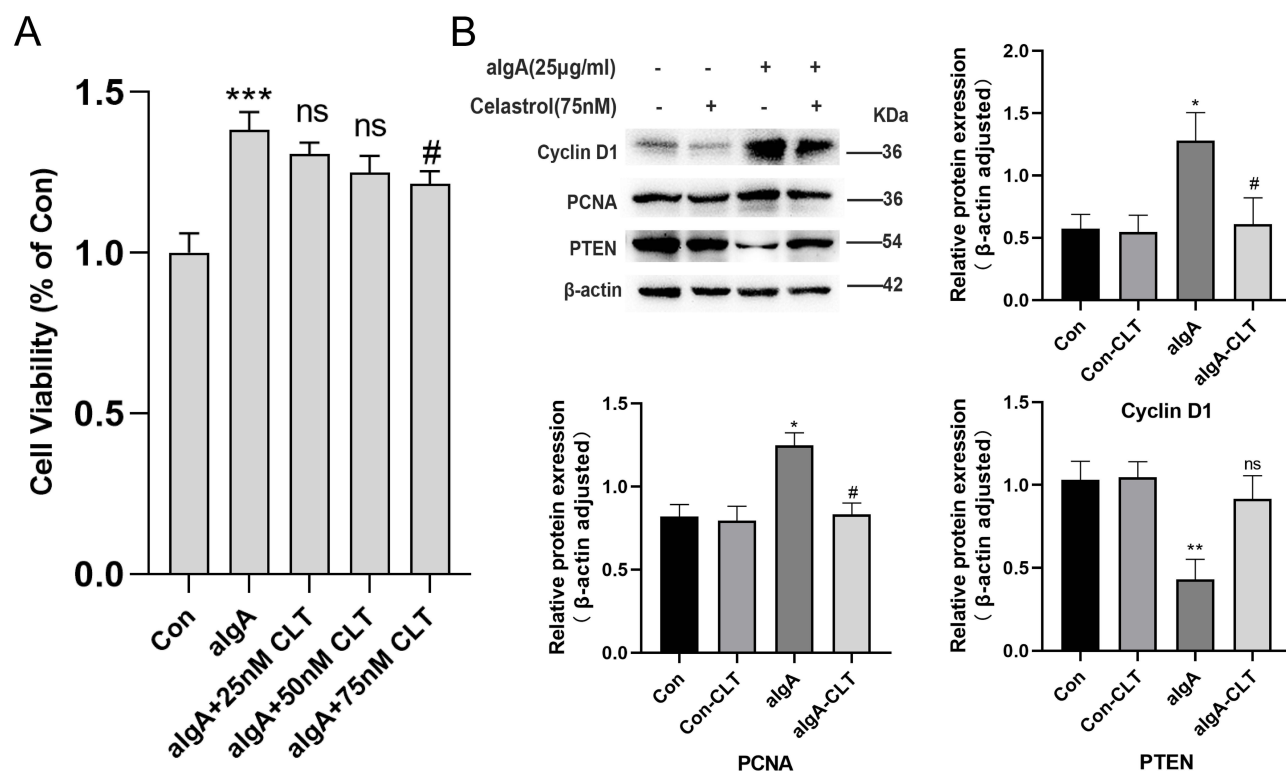


Figure 7 Celastrol inhibited HMCs proliferation and activated PTEN signaling. **(A)** The proliferation of HMCs with algA OR different concentrations of celastrol intervention was detected by CCK8 assay. **(B)** Western blot and gray value statistics of PTEN, Cyclin D1 and PCNA in HMCs. All data presented as mean \pm SD, $n=5$ OR 6. * $p < 0.05$ vs control group, ** $p < 0.01$ vs control group, *** $p < 0.001$ vs control group, # $p < 0.05$ vs algA group, ns: $p > 0.05$ vs Control OR algA group.

THH on IgAN. The component-target with the highest molecular docking fraction was chosen for experimental verification in vitro and in vivo.

In this study, 17 compounds were identified as active ingredients of the THH, and 165 common targets were identified between the active ingredients of THH and IgAN through network pharmacology. Functional pathway enrichment analysis suggested that THH interfered with the Pathways in cancer, PI3K-Akt signaling pathway, and other pathways. In accordance with the PPI network, ten candidate key targets of THH against IgAN were screened. Among all the screened active ingredients, celastrol may regulate the greatest number of these key targets, including STAT3, TP53, MYC, JUN and PTEN. STAT3 is a transcription factor that can be activated by a multitude of upstream factors, was reported to be activated during renal injury and was involved in renal fibrosis.^{35,36} In an exome chip-based association study involving 3363 IgA nephropathy patients and 9879 healthy controls of Han Chinese ancestry, STAT3 was identified as a susceptible gene for IgAN that might modulate the immune response.³⁷ TP53 is a well-known tumor suppressor, which can induce cell cycle arrest, apoptosis, and autophagy. It plays a considerable role in renal injury and subsequent kidney repair.³⁸ MYC was reported to regulate mitochondrial metabolism and glycolysis to support repair after kidney injury.³⁹ Our research in the past shows that c-Jun N-terminal protein kinase (JNK)/JUN plays a crucial role in IgAN mesangial cell proliferation and renal lesions. After being intervened by TwHF in vivo and by Triptolide in vitro, p-JUN signal transduction was inhibited, and mesangial proliferation was improved.⁴⁰

Celastrol is considered one of the most active and widely studied components of THH.⁸ This traditional medicinal component was listed by Cell in 2007 as most likely to be developed as modern drugs.⁴¹ Celastrol has recently been proven to restrain cancers, obesity, and inflammation.^{22,42,43} Recent research has demonstrated that celastrol can treat CKD,⁴⁴ obesity-associated nephropathy⁴⁵ and mesangioproliferative glomerulonephritis⁴⁶ by acting as an anti-inflammatory agent and inhibiting the production of cytokines. Celastrol has also been shown to be effective in regulating insulin resistance and autophagy in diabetic nephropathy.⁴⁷ In addition, celastrol has also been reported to treat Lupus Nephritis by regulating T-cell immunity.⁴⁸ These studies of celastrol in the treatment of other glomerular diseases have greatly inspired our future

research. PTEN is generally considered to be significant for many cellular processes, especially in cellular proliferation.⁴⁹ In PTEN-deficient mice, the activation of related pathways promotes the proliferation of renal cells, increasing kidney volume.⁵⁰ Furthermore, previous research of our team confirmed the crucial role of PTEN inhibition in IgAN renal lesions and mesangial cell proliferation, inhibition of PTEN advanced proliferating cell nuclear antigen (PCNA) and cyclin D1 expression through phosphorylation of JUN, accelerating the proliferation of IgAN mesangial cells.⁵¹ Considering that celastrol was predicted to be the most important bioactive ingredient in the PPI network of THH against IgAN and PTEN ranked among the greatest results of binding with celastrol by molecular docking, in this study PTEN was verified as the target of celastrol in the treatment of IgAN in the animal model and cell model. Through this study, we found that celastrol may be a targeted activator of PTEN, which is a key gene for the proliferation of mesangial cells in IgAN nephropathy. It is of significance for clarifying the mechanism of IgAN therapy and the exploration of new drugs. So far as we know, this is the first report on the mechanism of celastrol in the treatment of IgAN.

The experiments showed that celastrol could diminish the proliferation of mesangial cells, advance the expression of PTEN, and reduce the expression of Cyclin D1 and PCNA significantly in vitro and in vivo, which verified the predicted results of network analysis and molecular docking. There were still some shortcomings in this study. Deeper experiments are needed to prove that PTEN is the target of celastrol. Moreover, given the limitations of network analysis and incomplete public database data, some other bioactive ingredients and target genes may have been missed in our analysis. Further research is required to verify the reliability of these conclusions.

Conclusion

To identify the molecular mechanisms and signaling pathways by which THH exerts its therapeutic benefits in IgAN, the network pharmacology approach, the molecular docking method, and experimental confirmation were used in the current study. Celastrol was considered the most important active ingredient in the THH against IgAN target network. According to molecular docking, PTEN is predicted to be the best result of binding with celastrol. The experiments in vivo and in vitro have demonstrated that activating PTEN by celastrol may play a pivotal role in THH-attenuated IgAN renal injury. This study provides a systematic and visual overview of the possibility of further mechanistic studies of THH against IgAN.

Abbreviations

IgAN, IgA Nephropathy; THH, *Tripterygium hypoglaucum* (Lév.) Hutch; ACEI, Angiotensin-converting enzyme inhibitor; Angiotensin receptor blocker (ARB); TwHF, *Tripterygium wilfordii* Hook F; TCMS, Traditional Chinese Medicine Systems Pharmacology Database; ADME, absorption, distribution, metabolism and excretion; OB, oral bioavailability; OMIM, Online Mendelian Inheritance in Man; GO, Gene Ontology; KEGG, Kyoto Encyclopedia of Genes and Genomes; PPI, Protein–Protein Interaction; MCC, Maximal Clique Centrality; PDB, Protein Data Bank; CLT, Celastrol; HMCs, Glomerular Mesangial Cells; DMSO, dimethyl sulfoxide; CCK8, Cell Counting Kit-8; BP, biological process; CC, cellular component; MF, molecular function; PCNA, proliferating cell nuclear antigen.

Acknowledgments

We sincerely appreciate the time and effort of all who contributed to this study.

Author Contributions

All authors made a significant contribution to the work reported, whether that is in the conception, study design, execution, acquisition of data, analysis and interpretation, or in all these areas; took part in drafting, revising or critically reviewing the article; gave final approval of the version to be published; have agreed on the journal to which the article has been submitted; and agree to be accountable for all aspects of the work.

Funding

This work was supported by the National Natural Science Foundation of China (82070737, 82270752 and 82270733). Scientific Research Key Project of Hunan Traditional Chinese Medicine Administration (2021040), and PRO.RUN Fund of the Nephrology Group of CEBM (KYS2021-03-02-7).

Disclosure

The authors declare that the research was conducted in the absence of any commercial or financial relationships that could be construed as a potential conflict of interest.

References

1. Xu X, Wang G, Chen N, et al. Long-term exposure to air pollution and increased risk of membranous nephropathy in China. *J Am Soc Nephrol.* 2016;27(12):3739–3746. doi:10.1681/ASN.2016010093
2. O'Shaughnessy MM, Hogan SL, Thompson BD, Coppo R, Fogo AB, Jennette JC. Glomerular disease frequencies by race, sex and region: results from the International Kidney Biopsy Survey. *Nephrol Dial Transplant.* 2018;33(4):661–669. doi:10.1093/ndt/gfx189
3. Lai KN, Tang SC, Schena FP, et al. IgA nephropathy. *Nat Rev Dis Primers.* 2016;2:16001. doi:10.1038/nrdp.2016.1
4. Rovin BH, Adler SG, Barratt J, et al. KDIGO 2021 clinical practice guideline for the management of glomerular diseases. *Kidney Int.* 2021;100(4s):S1–S276. doi:10.1016/j.kint.2021.05.021
5. Wang XH, Lang R, Liang Y, Zeng Q, Chen N, Yu RH. Traditional Chinese medicine in treating IgA nephropathy: from basic science to clinical research. *J Transl Int Med.* 2021;9(3):161–167. doi:10.2478/jtim-2021-0021
6. Law SK, Simmons MP, Techen N, et al. Molecular analyses of the Chinese herb Leigongteng (*Tripterygium wilfordii* Hook.f.). *Phytochemistry.* 2011;72(1):21–26. doi:10.1016/j.phytochem.2010.10.015
7. Zhang X, Li N, Yao Y, et al. Identification of species in *Tripterygium* (Celastraceae) based on DNA barcoding. *Biol Pharm Bull.* 2016;39(11):1760–1766. doi:10.1248/bpb.b15-00956
8. Zhao J, Zhang F, Xiao X, et al. *Tripterygium hypoglaucum* (Lévl.) Hutch and its main bioactive components: recent advances in pharmacological activity, pharmacokinetics and potential toxicity. *Front Pharmacol.* 2021;12:715359. doi:10.3389/fphar.2021.715359
9. Tong X, Qiao Y, Yang Y, et al. Applications and mechanisms of *Tripterygium wilfordii* Hook. F. and its preparations in kidney diseases. *Front Pharmacol.* 2022;13:846746. doi:10.3389/fphar.2022.846746
10. Jiang Y, Zhong M, Long F, Yang R. Deciphering the active ingredients and molecular mechanisms of *Tripterygium hypoglaucum* (Lévl.) Hutch against rheumatoid arthritis based on network pharmacology. *Evid Based Complement Alternat Med.* 2020;2020:2361865. doi:10.1155/2020/2361865
11. Li F, Han D, Wang B, et al. Topical treatment of colquhounia root relieves skin inflammation and itch in imiquimod-induced psoriasiform dermatitis in mice. *Mediators Inflamm.* 2022;2022:5782922. doi:10.1155/2022/5782922
12. Ma Z, Liu Y, Li C, Zhang Y, Lin N. Repurposing a clinically approved prescription Colquhounia root tablet to treat diabetic kidney disease via suppressing PI3K/AKT/NF- κ B activation. *Chin Med.* 2022;17(1):2. doi:10.1186/s13020-021-00563-7
13. Zhu B, Wang Y, Jardine M, et al. *Tripterygium* preparations for the treatment of CKD: a systematic review and meta-analysis. *Am J Kidney Dis.* 2013;62(3):515–530. doi:10.1053/j.ajkd.2013.02.374
14. Hopkins AL. Network pharmacology. *Nat Biotechnol.* 2007;25(10):1110–1111. doi:10.1038/nbt1007-1110
15. Wei TF, Zhao L, Huang P, et al. Qing-Yi decoction in the treatment of acute pancreatitis: an integrated approach based on chemical profile, network pharmacology, molecular docking and experimental evaluation. *Front Pharmacol.* 2021;12:590994. doi:10.3389/fphar.2021.590994
16. Su X, Kong L, Lei X, Hu L, Ye M, Zou H. Biological fingerprinting analysis of traditional Chinese medicines with targeting ADME/Tox property for screening of bioactive compounds by chromatographic and MS methods. *Mini Rev Med Chem.* 2007;7(1):87–98. doi:10.2174/138955707779317830
17. Amberger JS, Bocchini CA, Schiettecatte F, Scott AF, Hamosh A. OMIM.org: Online Mendelian Inheritance in Man (OMIM[®]), an online catalog of human genes and genetic disorders. *Nucleic Acids Res.* 2015;43(Database issue):D789–D798. doi:10.1093/nar/gku1205
18. Fishilevich S, Zimmerman S, Kohn A, et al. Genic insights from integrated human proteomics in GeneCards. *Database.* 2016;2016:baw030. doi:10.1093/database/baw030
19. Martino E, Chiarugi S, Margheriti F, Garau G. Mapping, structure and modulation of PPI. *Front Chem.* 2021;9:718405. doi:10.3389/fchem.2021.718405
20. Szklarczyk D, Gable AL, Lyon D, et al. STRING v11: protein-protein association networks with increased coverage, supporting functional discovery in genome-wide experimental datasets. *Nucleic Acids Res.* 2019;47(D1):D607–D613. doi:10.1093/nar/gky1131
21. Zhao L, Lan Z, Peng L, et al. Triptolide promotes autophagy to inhibit mesangial cell proliferation in IgA nephropathy via the CARD9/p38 MAPK pathway. *Cell Prolif.* 2022;55(9):e13278. doi:10.1111/cpr.13278
22. Pace S, Zhang K, Jordan PM, et al. Anti-inflammatory celestrol promotes a switch from leukotriene biosynthesis to formation of specialized pro-resolving lipid mediators. *Pharmacol Res.* 2021;167:105556. doi:10.1016/j.phrs.2021.105556
23. Xia M, Liu D, Tang X, et al. Dihydroartemisinin inhibits the proliferation of IgAN mesangial cells through the mTOR signaling pathway. *Int Immunopharmacol.* 2020;80:106125. doi:10.1016/j.intimp.2019.106125
24. Saikia S, Bordoloi M. Molecular docking: challenges, advances and its use in drug discovery perspective. *Curr Drug Targets.* 2019;20(5):501–521. doi:10.2174/1389450119666181022153016
25. O'Shaughnessy MM, Montez-Rath ME, Lafayette RA, Winkelmayer WC. Patient characteristics and outcomes by GN subtype in ESRD. *Clin J Am Soc Nephrol.* 2015;10(7):1170–1178. doi:10.2215/CJN.11261114
26. Huang X, Xu G. An update on targeted treatment of IgA nephropathy: an autoimmune perspective. *Front Pharmacol.* 2021;12:715253. doi:10.3389/fphar.2021.715253
27. Rodrigues JC, Haas M, Reich HN. IgA nephropathy. *Clin J Am Soc Nephrol.* 2017;12(4):677–686. doi:10.2215/CJN.07420716

28. Guo Y, Guo N, Wang J, Wang R, Tang L. Retrospective analysis of Tripterygium wilfordii polyglycoside combined with angiotensin receptor blockers for the treatment of primary membranous nephropathy with sub-nephrotic proteinuria. *Ren Fail.* 2021;43(1):729–736. doi:10.1080/0886022X.2021.1918555
29. Zhang H, Li X, Xu H, Ran F, Zhao G. Effect and safety evaluation of tacrolimus and tripterygium glycosides combined therapy in treatment of Henoch-Schönlein purpura nephritis. *Int J Urol.* 2021;28(11):1157–1163. doi:10.1111/iju.14665
30. Zhang M, Chen Y, Yang MJ, et al. Celastrol attenuates renal injury in diabetic rats via MAPK/NF- κ B pathway. *Phytother Res.* 2019;33(4):1191–1198. doi:10.1002/ptr.6314
31. Ma ZJ, Zhang XN, Li L, et al. Tripterygium glycosides tablet ameliorates renal tubulointerstitial fibrosis via the toll-like receptor 4/nuclear factor kappa B signaling pathway in high-fat diet fed and streptozotocin-induced diabetic rats. *J Diabetes Res.* 2015;2015:390428. doi:10.1155/2015/390428
32. He L, Peng X, Liu G, et al. Anti-inflammatory effects of triptolide on IgA nephropathy in rats. *Immunopharmacol Immunotoxicol.* 2015;37(5):421–427. doi:10.3109/08923973.2015.1080265
33. Gao Q, Shen W, Qin W, et al. Treatment of db/db diabetic mice with triptolide: a novel therapy for diabetic nephropathy. *Nephrol Dial Transplant.* 2010;25(11):3539–3547. doi:10.1093/ndt/gfq245
34. Tamouza H, Chemouny JM, Raskova Kafkova L, et al. The IgA1 immune complex-mediated activation of the MAPK/ERK kinase pathway in mesangial cells is associated with glomerular damage in IgA nephropathy. *Kidney Int.* 2012;82(12):1284–1296. doi:10.1038/ki.2012.192
35. Chen W, Yuan H, Cao W, et al. Blocking interleukin-6 trans-signaling protects against renal fibrosis by suppressing STAT3 activation. *Theranostics.* 2019;9(14):3980–3991. doi:10.7150/thno.32352
36. Cheng Y, Wang D, Wang F, et al. Endogenous miR-204 protects the kidney against chronic injury in hypertension and diabetes. *J Am Soc Nephrol.* 2020;31(7):1539–1554. doi:10.1681/ASN.2019101100
37. Zhou XJ, Tsoi LC, Hu Y, et al. Exome chip analyses and genetic risk for IgA nephropathy among Han Chinese. *Clin J Am Soc Nephrol.* 2021;16(2):213–224. doi:10.2215/CJN.06910520
38. Tang C, Ma Z, Zhu J, et al. P53 in kidney injury and repair: mechanism and therapeutic potentials. *Pharmacol Ther.* 2019;195:5–12. doi:10.1016/j.pharmthera.2018.10.013
39. Yakulov TA, Todkar AP, Slanchev K, et al. CXCL12 and MYC control energy metabolism to support adaptive responses after kidney injury. *Nat Commun.* 2018;9(1):3660. doi:10.1038/s41467-018-06094-4
40. Xia M, Liu D, Liu H, et al. Based on network pharmacology tools to investigate the mechanism of Tripterygium wilfordii against IgA nephropathy. *Front Med.* 2021;8:794962. doi:10.3389/fmed.2021.794962
41. Corson TW, Crews CM. Molecular understanding and modern application of traditional medicines: triumphs and trials. *Cell.* 2007;130(5):769–774. doi:10.1016/j.cell.2007.08.021
42. Liu J, Lee J, Salazar Hernandez MA, Mazitschek R, Ozcan U. Treatment of obesity with celastrol. *Cell.* 2015;161(5):999–1011. doi:10.1016/j.cell.2015.05.011
43. Chen X, Zhao Y, Luo W, et al. Celastrol induces ROS-mediated apoptosis via directly targeting peroxiredoxin-2 in gastric cancer cells. *Theranostics.* 2020;10(22):10290–10308. doi:10.7150/thno.46728
44. Wu Q, Wang J, Wang Y, et al. Targeted delivery of celastrol to glomerular endothelium and podocytes for chronic kidney disease treatment. *Nano Res.* 2022;15(4):3556–3568. doi:10.1007/s12274-021-3894-x
45. Sun Z, Li Y, Qian Y, et al. Celastrol attenuates ox-LDL-induced mesangial cell proliferation via suppressing NLRP3 inflammasome activation. *Cell Death Discov.* 2019;5:114. doi:10.1038/s41420-019-0196-0
46. Guo L, Luo S, Du Z, et al. Targeted delivery of celastrol to mesangial cells is effective against mesangioproliferative glomerulonephritis. *Nat Commun.* 2017;8(1):878. doi:10.1038/s41467-017-00834-8
47. Zhan X, Yan C, Chen Y, et al. Celastrol antagonizes high glucose-evoked podocyte injury, inflammation and insulin resistance by restoring the HO-1-mediated autophagy pathway. *Mol Immunol.* 2018;104:61–68. doi:10.1016/j.molimm.2018.10.021
48. Xiang G, Shi K, Wang J. Celastrol alleviates murine lupus nephritis via inducing CD4⁺Foxp3⁺ regulatory T cells. *Folia Histochem Cytobiol.* 2022;60(3):237–246. doi:10.5603/FHC.a2022.0020
49. Worby CA, Dixon JE. PTEN. *Annu Rev Biochem.* 2014;83:641–669. doi:10.1146/annurev-biochem-082411-113907
50. Chen JK, Nagai K, Chen J, et al. Phosphatidylinositol 3-kinase signaling determines kidney size. *J Clin Invest.* 2015;125(6):2429–2444. doi:10.1172/JCI78945
51. Li Y, Xia M, Peng L, et al. Downregulation of miR-214-3p attenuates mesangial hypercellularity by targeting PTEN-mediated JNK/c-Jun signaling in IgA nephropathy. *Int J Biol Sci.* 2021;17(13):3343–3355. doi:10.7150/ijbs.61274

Drug Design, Development and Therapy

Dovepress

Publish your work in this journal

Drug Design, Development and Therapy is an international, peer-reviewed open-access journal that spans the spectrum of drug design and development through to clinical applications. Clinical outcomes, patient safety, and programs for the development and effective, safe, and sustained use of medicines are a feature of the journal, which has also been accepted for indexing on PubMed Central. The manuscript management system is completely online and includes a very quick and fair peer-review system, which is all easy to use. Visit <http://www.dovepress.com/testimonials.php> to read real quotes from published authors.

Submit your manuscript here: <https://www.dovepress.com/drug-design-development-and-therapy-journal>